

## THE INFLUENCE OF CONSOLIDATION PROCEDURE PARAMETERS ON COMPACTION OF Al POWDER

LOWE Terry C.<sup>1</sup>, KUNČICKÁ Lenka<sup>2,3</sup>, KOCICH Radim<sup>2,3</sup>, DAVIS Casey F.<sup>1</sup>, HLAVÁČ Libor<sup>3</sup>, DVOŘÁK Jiří<sup>4</sup>

<sup>1</sup> *The George S. Ansell Department of Metallurgical & Materials Engineering, Colorado School of Mines, Golden, Colorado, USA*

<sup>2</sup> *VSB - Technical University of Ostrava, Faculty of Metallurgy and Materials Engineering, Department of Material Forming, Ostrava, Czech Republic, EU*

<sup>3</sup> *VSB - Technical University of Ostrava, Regional Materials Science and Technology Centre, Ostrava, Czech Republic, EU*

<sup>4</sup> *Institute of Physics of Materials of the AS CR, v.v.i., Brno, Czech Republic, EU*

### Abstract

The influence of different consolidation procedures on compaction of Al powders was evaluated. Powder preparation procedures consisted of selection of particle size distribution, cold isostatic pressing (CIP), and vacuum sintering. Processing parameters investigated included the number of compression steps, compression pressure, and sintering temperature and time. Densities of the samples after compression and also after sintering were measured and compared. The overall oxygen content was analysed using Energy Dispersive Spectroscopy. Phase composition was determined using X-ray. Microhardness measurements were performed to evaluate the degree of compaction. Double-step CIP at 200+300 MPa and subsequent sintering at 500 °C for 60 min produced the best combination of properties from all the consolidation technologies of Al particles. Of the particle size ranges studies, those with diameters between 20 and 45 µm produced the best results. Aluminum oxide was present in the structure after all the processing treatments.

**Keywords:** Aluminum powder, cold isostatic pressing, sintering, oxygen content, X-ray

### 1. INTRODUCTION

Aluminum is the basic material for most modern light weight structures. Nevertheless, mechanical properties of pure (commercial purity) Al are rather low. Therefore, methods to improve the properties are widely researched. Among the basic possibilities of improvement is alloying and refinement of the size of structural units [1, 2]. Refinement of structural units is favourable from the point of view of imparting a higher volume of grain boundaries (GBs) [3]. This mechanism contributes to strengthening, since GBs act as obstacles for movement of dislocations, as well enable higher plasticity, since when the grain size is small enough, grain boundary sliding deformation mechanisms become active. Achievement of fine structural units is easier when the original material already consists of small units, for example by using initial powder particles with small sizes, including nano-powders [4]. Alloying can be performed either using additions of other elements with the purpose of development of a strengthening mechanism, such as solid solution strengthening by Mg or precipitation strengthening by Mg and Si for Al-based alloys, or by addition of dispersed secondary particles to create metal matrix composites (MMCs) [3, 5]. One of the most favourable discontinuously reinforced aluminum MMCs is mixture of Al matrix and Al<sub>2</sub>O<sub>3</sub> particles. The Al matrix has sufficient plasticity and ductility, while the particles are strong and hard to be able to carry the load. Combination of the two above mentioned methods is especially favourable, since Discontinuous Reinforced Aluminum (DRA) composites are preferably fabricated using powder metallurgy and then possess the combination of all the above mentioned advantages.

This study is focused on investigation of fabrication of aluminum material from powder. The aim of this experiment was to find out optimal conditions for compaction of Al powder. However, in the initial conditions

all the particles are covered with a thin layer of  $\text{Al}_2\text{O}_3$ . Therefore, there is a presupposition that it would be difficult to eliminate all the original oxides. However, a small amount of residual  $\text{Al}_2\text{O}_3$  can act as a reinforcing element. The factors evaluated during this experiment were the influence of particle size, compaction pressure, sintering time and sintering temperature. All the specimens processed with different further described technologies were cut into slices, which were subsequently subjected to several analyses.

## 2. EXPERIMENT

The selected particle size ranges were 25-45  $\mu\text{m}$ , 65-125  $\mu\text{m}$  and a 50:50 mixture of the two ranges. From each one of these ranges, three different samples intended to be subsequently subjected to different compaction procedures were prepared.

All the compaction was performed using cold isostatic pressing (CIP), as follows: pressurizing at 200 MPa for 30 seconds dwell and continuous depressurization; pressurizing at 300 MPa for 30 seconds dwell and continuous depressurization; and the subsequent combination of the afore mentioned (200 MPa for 30 seconds and 300 MPa for 30 seconds). All the samples were compressed in a die with an inner diameter of 20 mm, while the height of the powder filled in the die was 30 mm. The diameters of the compacted specimens were 18 mm.

The compressed samples were then cut using a water jet cutter. Electro wire cutting could not be applied, due to the surface aluminum oxides, which made the samples non-conductive. Each of the samples was sliced into 4 thin specimens. Three of the sliced specimens were subsequently processed with three different sintering heat treatments. The fourth sliced specimen from each of the compressed samples was maintained in the compressed condition as a reference specimen. As for the sintering parameters, two different temperatures (500 °C and 550 °C) and times (30 and 60 minutes) were chosen. The sintering conditions were then 500 °C for 30 minutes, 500 °C for 60 minutes, and 550 °C for 30 minutes.

After having performed all the compression and sintering, the specimens were analysed. All the 36 specimens were subjected to measurements of density. The measurements were performed ten times for each specimen and an average value was used as the final resulting value. Moreover, the three fine-particle specimens were subjected to X-ray analyses of chemical composition. Eventually, line microhardness analyses were randomly performed 5 times along the width of a specimen in order to investigate possible inhomogeneities throughout the circular specimens originating from the compression procedure. Average microhardness was the calculated for the samples compressed from the fine particles.

The chemical composition of the initial powder was determined by EDX analysis using scanning electron microscope (SEM) at VSB - Technical University of Ostrava (TUO), while microstructural observations were performed at Colorado School of Mines (CSM), CO, USA. Samples were mechanically polished and eventually ion milled with a JEOL CP Cross Section Polisher. All the compressing was performed on a CIP device located at TUO, while sintering was performed in a Zwick vacuum creep testing furnace at ASCR, Brno. Analyses of density were performed by an AccuPyc II Micromeritics pycnometer device at TUO. The X-ray analyses were performed using the Philips X'Pert system at CSM. Copper with  $\text{K}\alpha_1$  wavelength of 0.154054 nm and  $\text{K}\alpha_2$  wavelength of 0.154439 nm was used as the X-ray source. Final microhardness measurements were performed using a Vickers microhardness measuring device at CSM. The samples were loaded with the load of 500 g for 10 seconds. The line measurements were performed with 1 mm spacing starting 0.5 mm from the edge of a sample.

## 3. RESULTS AND DISCUSSION

### 3.1. Density and oxygen content

The chemical composition of the initial powder was as follows: 96.07 wt.% Al and 3.93 wt.% O. From the particle size point of view, the results of density measurements showed that the best compaction was achieved

for the specimens consisting only of the finest grain size range (25-45  $\mu\text{m}$ ) for all the compression procedures. This finding is in accordance with conclusions ensuing from the study by Eldesouky et al. [6], who investigated relative density of samples consolidated from AA2124 aluminum powder. They achieved the best results for the fraction at the size of 40  $\mu\text{m}$ .

As for the compression pressure, the best results were achieved for the specimens compressed by the double-pressing technology (an example of the compressed samples is shown in **Fig. 1**). This conclusion applies for all the sintering temperatures and times. The sintering parameters were selected according to the studies performed by Sweet et al. [7], Liu et al. [8] and Dadbakhsh et al. [9]. The 30 minutes sintering time was also chosen based on study of literature [10]. The sintering procedure with the longer time was designed for the lower temperature in order to evaluate possible differences between the properties of specimens after the lower temperature + longer time and higher temperature + shorter time sintering procedures.

Results of density measurements for six specimens with the highest density are summarized in **Table 1**. However, as can be seen in the table, all the measured densities were slightly higher than the theoretical density of pure aluminum (2.70  $\text{g}\cdot\text{cm}^{-3}$ ). This can be a consequence of the presence of oxygen and therefore aluminum oxides. Aluminum oxides have higher theoretical density than pure aluminum. For example, the most common aluminum oxide,  $\text{Al}_2\text{O}_3$ , has the average density of 3.95  $\text{g}\cdot\text{cm}^{-3}$  [3]. Therefore, EDX analyses of oxygen contents were performed five times for each specimen and mean average values were subsequently calculated. The results of EDX chemical composition analyses of the selected specimens are also shown in **Table 1**, while SEM microstructure of sample 2 (see **Table 1**) is depicted in **Fig. 2**.

**Table 1** Densities and oxygen contents for selected specimens

sample number	particles fraction ( $\mu\text{m}$ )	CIP (MPa)	sintering temperature ( $^{\circ}\text{C}$ )	sintering time (min)	oxygen content (wt. %)	measured density ( $\text{g}\cdot\text{cm}^{-3}$ )	calculated density with $\text{Al}_2\text{O}_3$ ( $\text{g}\cdot\text{cm}^{-3}$ )
1	fine	200+300	500	30	5.70 $\pm$ 0.03	2.8276	2.851
2	fine	200+300	500	60	4.97 $\pm$ 0.19	2.8073	2.832
3	fine	200+300	550	30	5.65 $\pm$ 0.24	2.8278	2.850
4	coarse	200	500	30	4.34 $\pm$ 0.11	2.8102	2.815
5	coarse	200	500	60	4.33 $\pm$ 0.29	2.8944	2.815
6	mixture	200+300	500	30	4.51 $\pm$ 0.07	2.8229	2.819

The EDX analyses results showed presence of oxygen in all the analysed specimens; with oxygen levels between 7 and 10 at.%. The source of the oxygen is probably the protective aluminum oxide layer, which initially coated the surface of all the particles. This supposition is supported by the fact that the content of oxygen is the highest for the specimens prepared from the finest particles, for which the surface to volume ratio is higher than for coarser particles. Therefore the overall percentage content of oxygen for fine particles is higher than for larger particles. During the compression itself, the oxides already present at the surfaces of the particles get cracked and some of them can possibly be turned into hydroxides, which subsequently get evaporated during sintering. However, the compression procedure does not seem to have any significant influence on the content of oxygen in the structures. From the point of view of sintering temperature, the oxygen content is lower for specimens sintered for the longer time of 60 minutes. Nevertheless, the evaporation/dissolution temperatures for Al oxides are very high (over 2000  $^{\circ}\text{C}$ ) and therefore they cannot be eliminated completely by the treatments [11]. To support the above mentioned presupposition that the increased density is caused by the presence of aluminum oxide, theoretical density calculations were performed. The results of all the confirmatory computations are summarized in **Table 1**.



**Fig. 1** Photo of a compressed sample (25-45  $\mu\text{m}$ , 200+300 MPa)

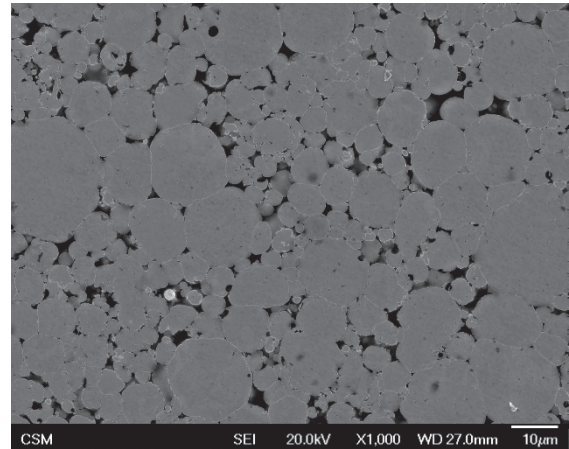


**Fig. 2** Microstructure of sample 25-45  $\mu\text{m}$ , 200+300 MPa, 500 °C/60 min

As the final analysis, the three fine-particle specimens were subjected to X-ray analyses of chemical composition. Such analyses will be helpful for identification of presence of phases in the structures of the specimens. The results of the X-ray analyses were comparable for all the three investigated specimens. By this reason, only the results for specimen 2, which has been proven to be processed in the most favourable way, will be presented here. X-ray data plot for specimen 2 is depicted in **Fig. 3**.

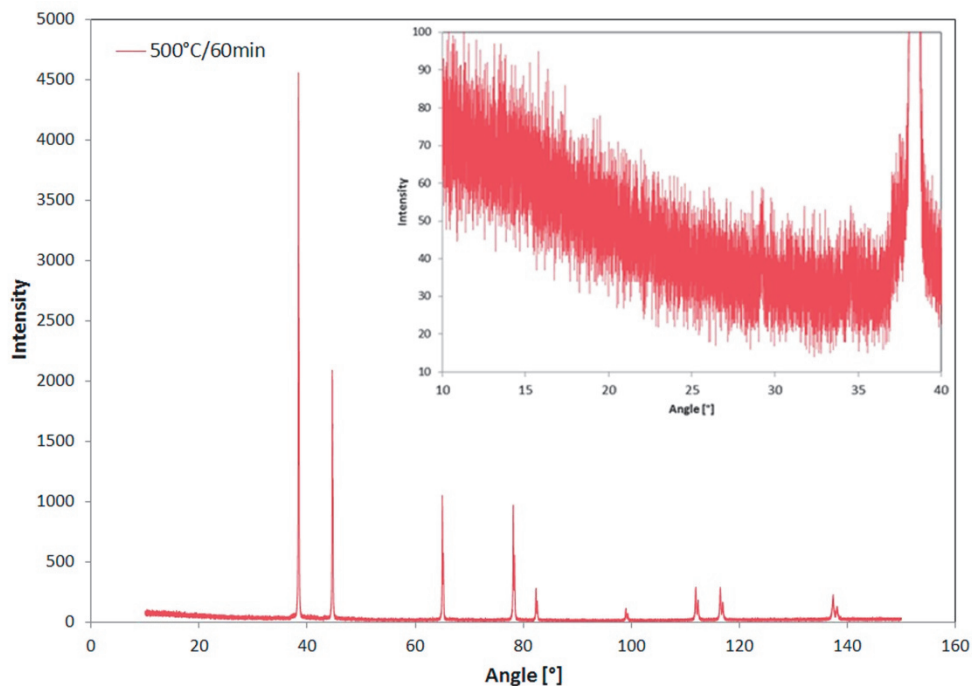


**Fig. 3** X-ray plot of chemical composition for specimen 2

The most distinctive peaks in the plot are peaks corresponding to pure Al phase. Nevertheless, noticeable is the beginning of the plotted dependence, the detail of which is depicted in the upper right corner of **Fig. 3**. In a reference plot of X-ray data for pure  $\text{Al}_2\text{O}_3$ , a set of distinctive peaks starts to rise at the angle of  $28^\circ$  (not shown here). Although the low intensities in the plot of specimen 2 are burdened with noise, a slight increase forming a little local peak can be distinguished between the angle of  $28^\circ$  and  $29^\circ$ . This is most probably due to

the presence of Al<sub>2</sub>O<sub>3</sub>. In the detail in **Fig. 3** can also be seen that the plotted data exhibit a slight increase towards lower angles. Such a course of X-ray data indicates a presence of amorphous phase. Since the above described observations of distinctive peaks are valid only for crystalline structures, it is probable that Al<sub>2</sub>O<sub>3</sub> will be present in the structure in an amorphous state. X-ray analyses are not able to provide exact determination of chemical composition of amorphous phases. Nevertheless, bringing together all the results from the above described measurements, analyses and calculations, the amorphous phase is most probably Al<sub>2</sub>O<sub>3</sub>.

### 3.2. Microhardness

As the final part of this investigation, microhardness measurements were performed. The above mentioned analyses have already proven the superior performance of finer particle size range subject to the 200+300 MPa double step compression procedure. According to the oxygen content results, the most suitable sintering procedure seems to be 500 °C for 60 minutes. For all the specimens, the measurements were performed 5 times and average values were calculated. The results, summarized in **Table 2**, prove the above mentioned conclusion and complete a comprehensive idea about a suitable pre-compaction procedure.

**Table 2** Microhardness measurements results

Sample number	1	2	3
Microhardness [HV]	26.33 ± 1.15	27.40 ± 1.96	29.58 ± 2.07

The results of the line measurements are demonstrated in **Fig. 4**, in which they are comparatively scaled to the average value of each of the measurements set as 1. As can be seen from the figure, no increasing/decreasing trend in microhardness towards the central part of the samples has been observed. Therefore, the samples can be considered to be homogeneously compacted.

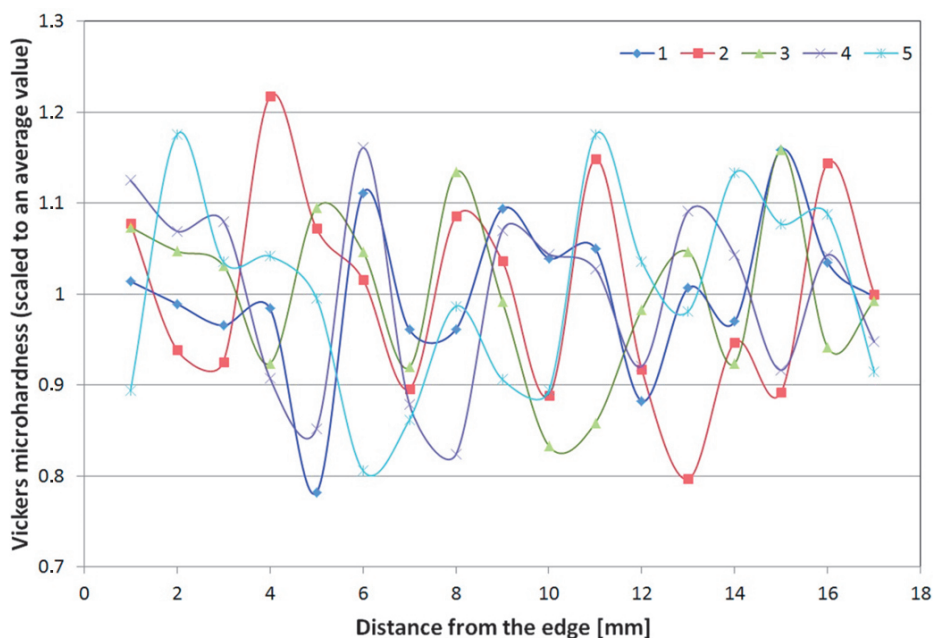


**Fig. 4** Results of random line microhardness measurements

## 4. CONCLUSIONS

We have shown that higher extent of compaction can be achieved when fine size particles are used (25 - 45 µm - mesh 325). Furthermore, cold isostatic pressing with two steps has a higher compacting efficiency than one step pressing. This was the case for both the analysed one-step procedures - 200 MPa and 300 MPa.

Density measurements showed density values higher than theoretical for pure aluminum for all the specimens. Nevertheless, SEM as well as X-ray analyses both showed the presence of higher density aluminum oxides. Microhardness measurements confirmed the above mentioned conclusions and prior presuppositions. The specimens consisting of the finest particles compressed in two steps all have the highest microhardness values. Microhardness analyses further did not prove any increasing/decreasing trend when measured throughout the cross-section of a specimen. Residuals of alumina within the compressed and sintered samples can be favourable for mechanical properties of the material, since they can contribute to strengthening of the final material.

## ACKNOWLEDGEMENTS

*This paper was created within the research project no. SP2015/89 of VSB - Technical University of Ostrava and the Project No. LO1203 "Regional Materials Science and Technology Centre - Feasibility Program" funded by Ministry of Education, Youth and Sports of the Czech Republic.*

## REFERENCES

- [1] MOKHNACHE E.O., WANG G., GENG L., KAVEENDRAN B., HUANG L. Synthesis and Characterization of In Situ (Al<sub>2</sub>O<sub>3</sub>-Si)/Al Composites by Reaction Hot Pressing. *Acta Metallurgica Sinica (English Letters)*, Vol. 27, No. 5, 2014, pp. 930-936.
- [2] ASHIDA M., HORITA Z. Effects of ball milling and high-pressure torsion for improving mechanical properties of Al-Al<sub>2</sub>O<sub>3</sub> nanocomposites. *Journal of Materials Science*, Vol. 47, No. 22, 2012, pp. 7821-7827.
- [3] RUSSELL A., LEE K.L. *Structure-Property Relations in Nonferrous Metals*. Wiley; n.d, New Jersey, 2005.
- [4] FAN G., XU R., TAN Z., ZHANG D., LI Z. Development of Flake Powder Metallurgy in Fabricating Metal Matrix Composites: A Review. *Acta Metallurgica Sinica (English Letters)*, Vol. 27, No. 5, 2014, pp. 806-815.
- [5] GHOSH K.S., GAO N., STARINK M.J. Characterisation of high pressure torsion processed 7150 Al-Zn-Mg-Cu alloy. *Materials Science and Engineering A*, Vol. 552, 2012, pp. 164-171.
- [6] ELDESOUKY A., JOHANSSON M., SVENGREN H., ATTALLAH M.M., SALEM H.G. Effect of grain size reduction of AA2124 aluminum alloy powder compacted by spark plasma sintering. *Journal of Alloys Compounds*, Vol. 609, 2014, pp. 215-221.
- [7] SWEET G.A., BROCHU M., HEXEMER R.L., DONALDSON I.W., BISHOP D.P. Microstructure and mechanical properties of air atomized aluminum powder consolidated via spark plasma sintering. *Materials Science and Engineering A*, Vol. 608, 2014, pp. 273-282.
- [8] LIU Z., ZHANG Z., LU J., KORZNIKOV A.V., KORZNIKOVA E., WANG F. Effect of sintering temperature on microstructures and mechanical properties of spark plasma sintered nanocrystalline aluminum. *Materials & Design*, Vol. 64, 2014, pp. 625-630.
- [9] DADBAKSH S., HAO L. Effect of hot isostatic pressing (HIP) on Al composite parts made from laser consolidated Al/Fe<sub>2</sub>O<sub>3</sub> powder mixtures. *Journal of Materials Processing Technology*, Vol. 212, No. 11, 2012, pp. 2474-2483.
- [10] BIDULSKÁ J., KVAČKAJ T., KOČIŠKO R., BIDULSKÝ R., GRANDE M.A., DONIČ T., et al. Influence of ECAP-Back Pressure on the Porosity Distribution, *Acta Physica Polonica A*, Vol. 117, No. 5, 2010, pp. 864-868.
- [11] GUO N., LUAN B., HE F., LI Z., LIU Q. Influence of flake thickness on the shape and distribution of Al<sub>2</sub>O<sub>3</sub> particles in Al matrix composites fabricated by flake powder metallurgy. *Scripta Materialia*, Vol. 78-79, 2014, pp. 10-13.